Magnetic Resonance Imaging 63 (2019) 12–20

Contents lists available at ScienceDirect

Magnetic Resonance Imaging

journal homepage: www.elsevier.com/locate/mri

Original contribution

Characterization of lower limb muscle activation patterns during walking and running with Intravoxel Incoherent Motion (IVIM) MR perfusion imaging

Pia M. Jungmann[a,b,*], Christian Pfirrmann[a], Christian Federau[a,c,d]

[a] Department of Radiology, Balgrist University Hospital, University of Zurich, Forchstrasse 340, 8008 Zurich, Switzerland
[b] Department of Diagnostic and Interventional Radiology, Medical Center - University of Freiburg, Faculty of Medicine, University of Freiburg, Germany
[c] Division of Diagnostic and Interventional Neuroradiology, Department of Radiology, University Hospital Basel, Petersgraben, 4031 Basle, Switzerland
[d] Institute for Biomedical Engineering, ETH Zürich und University of Zürich, Gloriastrasse, 35 8092 Zürich, Switzerland

ARTICLE INFO

Keywords:
Magnetic resonance imaging
Skeletal muscle
Perfusion imaging
Rest
Running

ABSTRACT

Background: The distribution of energy use among different lower limb muscles during walking and running is not well understood. Local blood flow within skeletal muscle tissue depends on its metabolic activity during activation. The non-invasive magnetic resonance microvascular perfusion method Intravoxel Incoherent Motion (IVIM) is able to quantify muscle activation.

Purpose: To non-invasively determine quantitative changes in local microvascular perfusion and blood flow via IVIM in order to characterize specific muscle activation of the lower limb at rest, during walking and during running.

Methods: 3 T MR IVIM diffusion-weighted images of $N = 16$ lower extremities (bilateral imaging of $n = 8$ healthy volunteers; mean age 27.5 ± 5.7 years) were acquired at rest and immediately after walking and running for 15 min, respectively. A transverse monopolar pulsed gradient fat suppressed spin echo EPI sequence was used (9 b-values from 0 to 1000s/mm^2, 3 orthogonal directions). Anatomical transverse T1-weighted turbo SE images were acquired at rest. Muscles at the pelvis, thigh and lower leg were segmented. IVIM perfusion parameters f, D* and fD* and the diffusion coefficient D were obtained after standard two-steps fitting of the IVIM bi-exponential signal equation. Descriptive statistics, *t*-tests, Pearson's correlations and Partial Spearman correlations were used for statistical analyses.

Results: The microvascular blood flow (fD*) increased significantly and stepwise from rest ($1.65 \pm 0.83*10^{-3}$ mm^2/s) to walking ($1.99 \pm 0.80*10^{-3}$ mm^2/s, $P < 0.001$) and running ($2.18 \pm 0.98*10^{-3}$ mm^2/s, $P < 0.001$). The perfusion increase was most pronounced for lower leg and feet muscles ($P < 0.001$). Hamstring muscles showed a higher microvascular perfusion increase than quadriceps muscles ($P < 0.05$). A higher increase of the heartrate from walking to running correlated significantly with a lower increase of fD* from walking to running ($R = -0.16$, $P = 0.001$).

Conclusion: IVIM MRI quantitatively measures local microvascular muscle perfusion to detect muscle activation patterns through walking and running. A redistribution of blood flow towards the lower leg was observed during running as compared to walking.

1. Introduction

The mechanics of human walking and running are known to differ. During walking, the body acts like an inverted pendulum, that swings along step by step. During walking, at least one foot is in contact with the ground at any given time. Running is characterized by a bouncing gait: during the first half of the step, mechanical energy is absorbed to slow down and lower the body, during the second half of the step, energy is released to lift and accelerate the body. During running, the time of foot contact to the ground is minimal. For a small period, neither of the feet is in contact with the ground. Knees are lifted up to a higher degree during running as compared to walking. Walking is associated with first striking the heel, whereas running with higher speed involves landing on the midfoot or forefoot.

* Corresponding author at: Department of Radiology, Balgrist University Hospital, University of Zurich, Forchstrasse 340, 8008 Zurich, Switzerland.
E-mail addresses: pia.jungmann@uniklinik-freiburg.de (P.M. Jungmann), christian.pfirrmann@balgrist.ch (C. Pfirrmann), federau@biomed.ee.ethz.ch (C. Federau).

https://doi.org/10.1016/j.mri.2019.07.016
Received 5 April 2019; Received in revised form 10 July 2019; Accepted 25 July 2019

The mechanics of human legged locomotion involve many muscles with various mechanical function. Surprisingly, little is known on the specific distribution of energy use among the individual skeletal muscles in vivo, which might be due to a lack of methodology permitting non-invasive assessment of muscular activation patterns.

Direct measurements of the oxygen consumption of individual muscle using the arteriovenous oxygen difference (Fick method) are not realistic, as they require sampling of the inflowing arterial blood and of the outflowing venous blood in order to determine the oxygen content and calculate the muscle specific oxygen use. Electromyography (EMG) measures the recruitment of active muscle fibers [1]. It has the limitation that simultaneous recording of a several muscles at the same time is tedious: Non-invasive EMG with surface electrodes is not entirely muscle specific and performing intramuscular EMG of several muscles simultaneously is very invasive and inconvenient for the subject. Further, EMG results do not correlate directly with quantitative metabolic use [1]. Marsh et al. suggested that the best technique for accurately assessing muscle energy use during locomotion is perfusion imaging [2]. The authors measured the distribution of radioactively labeled microspheres (size 15 μm, large enough to lodge in the systemic capillaries). The quantitative distribution of the fraction of blood correlated with the energy consumption of the individual muscle during locomotion. Obviously, the use of this method in healthy humans is ethically not acceptable.

Magnetic resonance (MR) imaging allows to assess muscle composition and perfusion in a non-invasive manner. T2 relaxation time measurements have been used to estimate the volume of muscle that was active during a preceding exercise. Further, an increase in the long component of bi-exponential T2 with exercise was observed in different studies [3,4]. This finding may be caused by an increased blood flow or muscle edema due to local inflammation after exercise [5–7]. Still, these measurements are not able to provide information on the quantitative amount of energy used [1,8]. An MR technique that aims to determine muscle perfusion is dynamic contrast-enhanced T1-weighted MR imaging [9]. Disadvantages are the need of intravenous contrast injections and small regions of interest. Also, due to the contrast media injection the measurements cannot be repeated several times in a short time period. Arterial spin labeling is an MR perfusion technique that does not require contrast injection. However, this method is anatomically limited to regions with simple vascular anatomy [10]. Intravoxel Incoherent Motion (IVIM) is a perfusion MR imaging technique that is based on non-invasive local diffusion measurements. A good reproducibility of IVIM measurements was demonstrated previously [11]. The IVIM parameters are f, D, D* and fD*. The IVIM parameter f is the perfusion fraction. The IVIM parameters D and D* describe two mechanisms of incoherent motion on a voxel level in human tissue: D is the diffusion coefficient (order $10^{-3}\,mm^2/s$) representing the thermal molecular diffusion, and D* is the pseudo-diffusion coefficient (order $10^{-2}\,mm^2/s$) representing the microcirculation of blood in the capillary network (perfusion). fD* is a blood flow related parameter which is the multiplication of f and D* on a voxel-by-voxel basis. IVIM may be applied for whole body imaging [12,13]. While initially developed for the evaluation of brain tissue [14–17], IVIM has recently been applied successfully in several skeletal muscle perfusion studies [12,17–21]. IVIM provides microvascular perfusion information shortly after dedicated exercises, performed inside or outside the MR scanner [20–22]. Selectivity to a specific muscle exercise [20] and proportionality to the muscle effort [21] were demonstrated. Therefore, IVIM microvascular perfusion MRI seems to be an optimal technique to determine the local metabolic contribution of muscles during specific tasks. It permits quantitative, non-invasive local perfusion assessment of an entire limb.

The purpose of this study was to determine the IVIM parameters of the different muscles of the lower limb during walking and running in human.

2. Methods

2.1. Subjects

A total of $N = 16$ legs was assessed (bilateral legs of $n = 8$ healthy female volunteers; mean age ± SD of 27.5 ± 5.7 years). Inclusion criteria were normal range of motion of all joints at the lower leg and ability to run for 15 min on a treadmill. Exclusion criteria were clinical symptoms at any joint of the lower leg including pain, instability or blocking phenomena. Further exclusion criteria were general health conditions that prohibited running for 15 min (e.g. cardiovascular diseases) and MR contraindications such as pacemaker or pregnancy. The study protocol, amendments and informed consent documentation were reviewed and approved by the local institutional review boards. The study has been conducted according to the principles expressed in the Declaration of Helsinki. All volunteers gave informed consent to this work after the nature of the study, the study sequence, the walking and running tasks and the required MR scans had been fully explained.

2.2. Experimental design

The study sequence was as follow: first, the volunteers had to rest for 15 min in a lying position on the MR scanner table in order to relax all muscles. After these 15 min a first MR scan (“rest”) was obtained. Following, volunteers had to walk on the treadmill at a fix speed of 6 km/h for 15 min and continued to walk back to the MR scanner (about 1 min walk). Then the second MR scan (“walking”) was acquired immediately. After the second scan, volunteers had to run on the treadmill for 15 min at a fix speed of 10 km/h, or 9 km/h if 10 km/h was too fast for the volunteer. The volunteers continued running back to the MR scanner (about 40 s run). Following, the third (last) MR scan (“running”) was acquired immediately.

2.3. Walking and running task

Walking was defined as continuous motion with continuous contact to the ground (one foot had to be in contact with the ground at all times). Running was defined as intermittent loss of contact to the ground of both feet. During the walking and running task, the heartrate was continuously monitored. All volunteers had previous experience with treadmill running, therefore only minor instructions were required. Walking and running was performed without grabbing the handle bar. Speed was kept up for the entire task.

2.4. MR image acquisition

MR images from lower thoracic region to the toes were acquired on a 1.5 T scanner (Siemens Avanto Fit, Erlangen, Germany) using an 18-channel whole body coil. The acquisition was performed in the transverse plane in 5 to 6 blocks. Image stacks were appended for image analyses. An anatomical transverse T1-weighted turbo spin-echo (SE) sequence was acquired at rest. Identical IVIM diffusion-weighted images were acquired at rest, after walking and after running, respectively, using a standard monopolar pulsed gradient fat suppressed SE EPI sequence, with 9 b-values (0, 50, 100, 150, 200, 400, 600, 800, 1000 s/mm^2) acquired in 3 orthogonal directions. Further sequence parameters were: TR = 3100 ms, TE = 73 ms, bandwidth 2490 Hz/pixel, slice thickness 10 mm, acquisition matrix 134 × 92, FOV 274 × 399 mm. Time for the acquisition of one full set of IVIM images of the lower limb was 8 min 32 s (5 blocks) or 10 min 14 s (6 blocks).

2.5. Postprocessing

Using the Levenberg–Marquardt algorithm implemented in C++, the IVIM bi-exponential signal equation model was fitted in a standard two-steps procedure after pooling of the signal for each b value in the

full region of interest (ROI) as described previously [13,20]. For the quantitative analysis, first the signal of the full region of interest (ROI) was averaged for each b-value before performing the fitting procedure, as described previously [20,23]. The IVIM perfusion parameters f (perfusion fraction) and D* (pseudo-diffusion), as well as the diffusion coefficient D were calculated. For the parameter D, the curve was fitted for b $< 200\ s/mm^2$. Following, the curve was fitted for f and D* over all b-values, while keeping D constant. For the parameter fD* the parameters f and D* were multiplied scalar on a voxel-by-voxel basis. Finally, all images were convoluted with a rotationally symmetric Gaussian lowpass filter (size 10, standard deviation 3) [21].

2.6. MR image analysis

Manual segmentation of the muscles was performed using a custom designed graphical user interface programmed in Matlab (Mathworks, Natick, MA, USA) by one musculoskeletal radiologist (_BLINDED FOR REVIEW_, 10 years of experience). For segmentation of each entire muscle or muscle compartment, ROIs were drawn on all slices of the IVIM b0 images that showed the respective muscle, when necessary, with the help of the anatomical images acquired at rest. To determine quantitative values and changes in local diffusion and microvascular perfusion, the IVIM parameters f, D, D* and fD* were determined for each individual muscle/ muscle compartment. In the following, means were calculated for muscle groups (roman numerals) and muscle subgroups. The following muscles/ compartments were assessed for both legs of all volunteers (Fig. 1):

(i) Gluteal muscles and iliopsoas muscle: Iliopsoas muscle, gluteus maximus muscle, gluteus medius muscle, and gluteus minimus muscle
(ii) Thigh: tensor fascia lata muscle, major adductor muscle, long adductor muscle, short adductor muscle, vastus medialis, lateralis and intermedius muscle, rectus femoris muscle, short and long head of biceps femoris muscle, semimembranosus muscle, semitendinosus muscle, gracilis muscle, and sartorius muscle
(iii) Lower leg: anterior compartment, peroneal compartment, deep posterior compartment, medial and lateral gastrocnemius muscle, and soleus muscle
(iv) Foot: feet extensor muscles, feet flexor muscles.

Subgroups were additionally defined and analyzed as follow: Gluteal muscles included the gluteus maximus, medius and minimus. Adductor muscles included the major, short and long adductor muscle. The quadriceps included the rectus femoris muscle and the vastus medialis, laterals and intermedius muscles. Hamstrings included the semimembranosus, semitendinosus and biceps muscle.

2.7. Statistical analysis

Statistical analyses were performed with SPSS version 20.0.0 (SPSS Institute, Chicago, IL, USA) (-BLINDED FOR REVIEW-). All tests were performed based on a 0.05 level of significance. Mean values ± standard deviations (SD) were obtained for descriptive statistics. IVIM values (f, D, D*, fD*) were calculated as absolute values for each muscle/ muscle compartment, each muscle group and each muscle subgroup. Further, change of IVIM values from rest to walking, from rest to running and from walking to running was determined by calculating the percentage increase (%). Paired *t*-tests were used to compare quantitative IVIM parameters between the different groups (rest, walking, running). Independent samples t-tests were used to compare different muscle subgroups and muscle groups. Mean values ± SD, mean differences between groups and 95% confidence intervals (95% CI, lower value, upper value) were determined. Pearson correlations were calculated to assess correlations between IVIM values and IVIM change values with age and heartrate. Partial Spearman correlations were calculated to assess correlations of IVIM change with the increase of heartrate while controlling for age.

To calculate the required sample size, a retrospective power analysis (comparisons of matched pairs; student's sample *t*-test) was performed for important comparisons with statistically significant differences between the two groups. An alpha of 0.05, a power of 0.95 and a two-

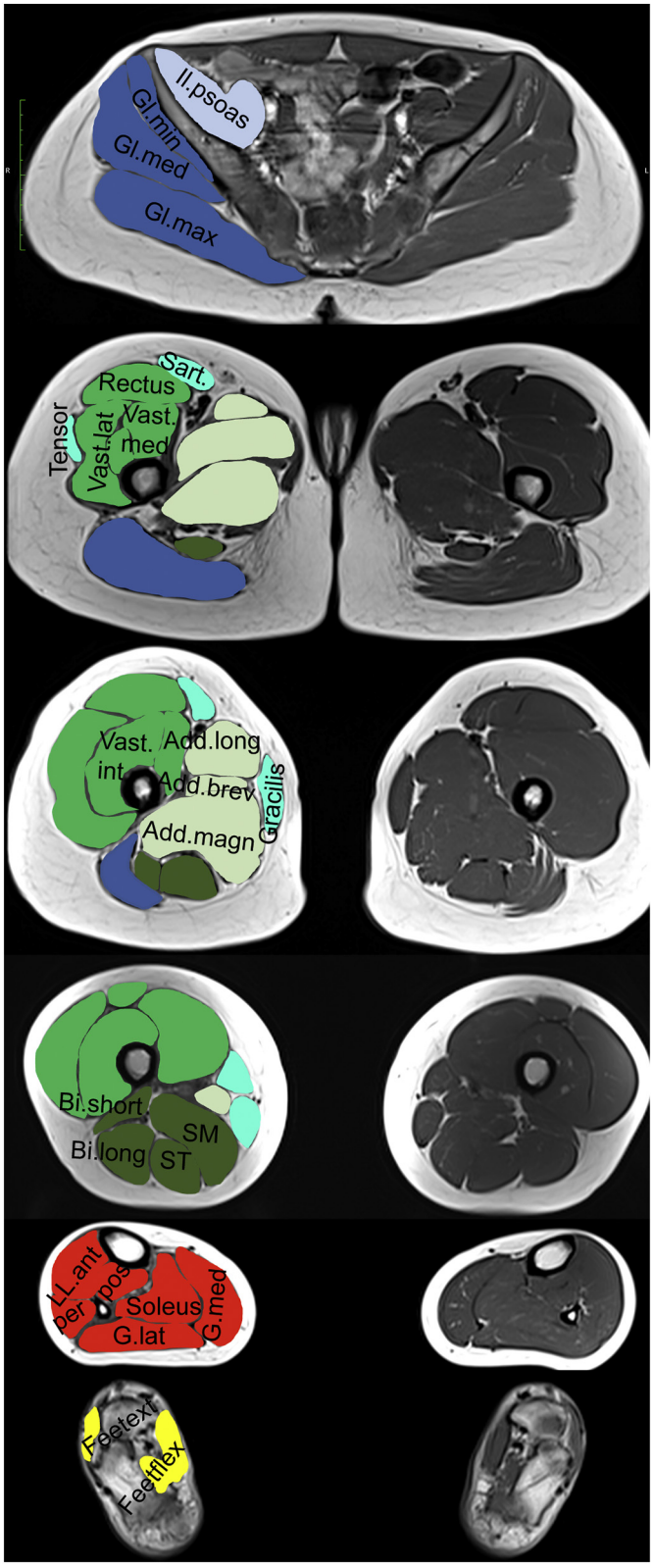

(caption on next page)

Fig. 1. Exemplary transverse T1-weighted slices that demonstrate muscle segmentation at the pelvis (A), thigh (B), lower leg (C) and foot (D). Regions of interest (ROIs) were drawn around muscles or muscle compartments on each slice. Dark blue: gluteal muscles; light blue: iliopsoas muscle; dark green: hamstrings; light green: adductor muscles; mint green: tensor fascia lata muscle, sartorius muscle, gracilis muscle; red: lower limb muscles; yellow: foot muscles. Il.psoas, Iliopsoas muscle; Gl.max., Gluteus maximus muscle; Gl.med, Gluteus medius muscle; Gl.min, Gluteus minimus muscle; Tensor, tensor fascia lata muscle; Add.magn, Adductor magnus muscle; Add.long, Adductor longus muscle; Add.brev, Adductor brevis muscle; Rectus, Rectus femoris muscle; Vast.med, Vastus medialis muscle; Vast.lat, Vastus lateralis muscle; Vast.int, Vastus intermedius muscle; SM, Semimembranosus muscle; ST, Semitendinosus muscle; Bi.long, long head of biceps muscle; Bi.short, short head of biceps muscle; Sartor., Sartorius muscle; Gracilis, Gracilis muscle; G.med., Gastrocnemius medialis muscle; G.lat., Gastrocnemius lateralis muscle; Soleus, Soleus muscle; LL.d.pos, lower leg deep posterior compartment; LL.ant, lower leg anterior compartment; LL.per, lower leg peroneal compartment; Feetext, feet extensor muscles; Feetflex, feet flexor muscles. (For interpretation of the references to colour in this figure legend, the reader is referred to the web version of this article.)

tailed test was used.

3. Results

3.1. Demographics

All 8 volunteers were able to complete the entire 15 min walking at 6 km/h, and the 15 min running (10 km/h for 6/8 subjects; 9 km/h for 2/8 subjects who were not able to run at 10 km/h for 15 min). The mean heartrate was 63 ± 3 bpm at rest, 113 ± 14 bpm during walking and 166 ± 14 bpm during running.

3.2. Global absolute IVIM perfusion parameters

For all IVIM perfusion parameters the mean value of all muscles increased stepwise and significantly from rest to walking and from walking to running (Table 1). The stepwise increase from rest ($1.65 \pm 0.83{\cdot}10^{-3}\,mm^2/s$) to walking ($1.99 \pm 0.80{\cdot}10^{-3}\,mm^2/s$, $P < 0.001$) and from walking to running ($2.18 \pm 0.98{\cdot}10^{-3}\,mm^2/s$, $P < 0.001$) was most pronounced for the IVIM blood flow related parameter fD*. Comparisons of absolute fD* values for each muscle or muscle group between rest, walking and running are shown in Fig. 2. Changes in fD* were most pronounced in the lower leg muscles (160.8% after walking and 237.3% after running relative to the fD* value at rest, $P < 0.001$) and in the foot muscles (178.4% and 281.4%, $P < 0.001$; Fig. 3). Exemplary curves of the relative IVIM decay and the corresponding bi-exponential fit of the soleus muscles at rest, after walking and after running are provided in Fig. 4. As for fD*, also for f and D* the increase was most pronounced in the lower leg muscles and/or foot muscles. A different behavior was observed in the thigh muscles: from rest to walking, an increase in fD* was observed ($P < 0.001$), while from rest to running a decrease was observed ($P < 0.001$). Also for the parameters f and D*, a decrease from walking to running was observed for the thigh muscles ($P < 0.001$ and $P = 0.079$, respectively). In contrast, the diffusion parameter D showed an increase also in the thigh muscles from walking to running (107.0%, $P < 0.001$), particularly at the hamstrings.

3.3. Specific findings at the thigh

In several muscles of the thigh fD* was higher after walking than at rest, but lower after running than at rest. Specifically, fD* was significantly lower after running as compared to rest in the hamstrings ($1.90 \pm 0.72{\cdot}10^{-3}\,mm^2/s$ versus $1.67 \pm 0.60{\cdot}10^{-3}\,mm^2/s$, $P = 0.001$) in the gluteus maximus muscles ($1.71 \pm 0.58{\cdot}10^{-3}\,mm^2/s$ versus $2.20 \pm 0.75{\cdot}10^{-3}\,mm^2/s$, $P = 0.018$), in the tensor fascia lata muscles ($1.80 \pm 0.61{\cdot}10^{-3}\,mm^2/s$ versus $2.00 \pm 0.73{\cdot}10^{-3}\,mm^2/s$, $P = 0.035$) and in the adductor muscles ($1.47 \pm 0.47{\cdot}10^{-3}\,mm^2/s$ versus $1.85 \pm 1.21{\cdot}10^{-3}\,mm^2/s$, $P = 0.300$). In the quadriceps muscles, fD* was non-significantly lower after running as compared to rest ($2.06 \pm 0.60{\cdot}10^{-3}\,mm^2/s$ versus $2.15 \pm 0.56{\cdot}10^{-3}\,mm^2/s$, $P = 0.197$).

3.4. Relative muscle perfusion changes

A higher fD* increase from rest to running was found for the hamstrings as compared to the opposing quadriceps muscles ($P = 0.033$; Table 2), for the vastus medialis muscles as compared to the vastus lateralis muscles ($P = 0.040$) and for the gastrocnemius medialis muscle as compared to the gastrocnemius lateralis muscle ($P = 0.041$).

3.5. Correlation analyses

Significant positive correlations were found for fD* at rest with fD* after walking ($R = 0.49$, $P < 0.001$) and for fD* after walking with fD* after running ($R = 0.41$, $P < 0.001$). Age showed an inverse correlation with fD* at rest ($R = -0.36$, $P < 0.001$), after walking ($R = -0.18$, $P = 0.001$) and after running ($R = -0.19$, $P < 0.001$). When controlling for age in Spearman correlation analyses, the heartrate during the respective activity showed significant negative correlations with fD* for rest ($R = -0.27$, $P < 0.001$), for walking ($R = -0.18$, $P < 0.001$) and for running ($R = -0.20$, $P < 0.001$). The change of fD* between the activities also showed an inverse correlation with the respective change of the heartrate ($P < 0.05$; Fig. 5).

3.6. Power analyses

In the retrospective power analysis, for the lower leg, the total sample size needed for comparisons of fD* between rest and running was 5. For f, D* and D the total sample sizes needed were 4, 11 and 6, respectively.

4. Discussion

This study demonstrates the detailed specific local activation patterns of lower limb muscles in human during walking and running, by using the ability to non-invasively measure local microperfusion with IVIM MRI. From rest to walking and from walking to running, an increase of the local blood flow towards the lower extremity was observed. Besides, a redistribution of the local blood within the lower leg regarding gluteal muscles, thigh, lower leg and foot muscles was found.

The overall muscle microvascular blood-flow of the lower extremity, described by the parameter fD*, increased stepwise and significantly from rest to walking and from walking to running. The increase of fD* from rest to walking for all muscle groups indicates, that all leg muscles contribute to gait movements. In a three-dimensional muscle-actuated model of the body a gait cycle dependency of the lower extremity muscle activation during walking, contributions of gluteal muscles, thigh muscles and lower leg muscles to walking were detected [24]. The contributions of the rectus femoris and hamstrings were described to be minor. This is in good accordance with our finding of only minor increases of fD* in the rectus femoris after walking. In contrast, the fD* increase was most pronounced at the lower leg and foot and from walking to running, which is in line with a stronger activation at the lower leg during running as reported by Anderson et al. [24]. Mastropietro et al. also found an increase in all IVIM parameters during isometric plantar flexion of the lower leg in the MR scanner, which is in line with our findings [22]. Still, they do not assess the effect of walking and running and the related distribution of muscle activation in the lower extremity. Interestingly, Mastropietro et al. report, that the IVIM

Table 1
IVIM values at rest, after walking and after running. Absolute mean blood-flow values ± SD, mean difference ± SEM between the groups including 95% confidence intervals (CI; lower value, upper value) and *P*-values for the comparisons of the groups are provided for the perfusion parameters fD*, f, D* and for the diffusion parameter D for all muscles, gluteal muscles and iliopsoas (gluteal), thigh muscles, lower leg muscles and foot muscles. P-values < 0.05 (in **bold**) are considered statistically significant.

	Absolute mean ± SD				Mean difference ± SEM (95% CI), P-value	
	Rest	Walking	Running	Walking vs rest	Running vs rest	Running vs walking
fD* ($*10^{-3}$)						
All muscles	1.65 ± 0.83	1.99 ± 0.80	2.18 ± 0.98	0.34 ± 0.04 (0.26, 0.42), **P < 0.001**	0.53 ± 0.06 (0.41, 0.65), **P < 0.001**	0.19 ± 0.05 (0.09, 0.28), **P < 0.001**
Gluteal	2.07 ± 0.73	2.18 ± 0.63	2.10 ± 0.65	0.11 ± 0.15 (−0.18, 0.41), *P* = 0.435	0.03 ± 0.15 (−0.28, 0.34), *P* = 0.835	−0.08 ± 0.12 (−0.32, 0.15), *P* = 0.477
Thigh	1.88 ± 0.77	2.02 ± 0.64	1.84 ± 0.67	0.15 ± 0.07 (0.01, 0.29), **P = 0.042**	−0.36 ± 0.83 (−0.19, 0.12), *P* = 0.650	−0.18 ± 0.05 (−0.29′8, −0.08), **P < 0.001**
Lower leg	1.02 ± 0.36	1.64 ± 0.77	2.42 ± 0.98	0.62 ± 0.09 (0.44, 0.79), **P < 0.001**	1.40 ± 0.13 (1.24, 1.65), **P < 0.001**	0.78 ± 0.11 (0.56, 1.00), **P < 0.001**
Foot	1.02 ± 0.45	1.82 ± 0.66	2.87 ± 0.18	0.80 ± 0.19 (0.40, 1.19), **P = 0.001**	1.85 ± 0.29 (0.44, 1.67), **P < 0.001**	1.06 ± 0.39 (0.44, 1.67), **P = 0.002**
D ($*10^{-3}$)						
All muscles	1.20 ± 0.18	1.24 ± 0.19	1.28 ± 0.20	0.036 ± 0.006 (0.025, 0.048), **P < 0.001**	0.077 ± 0.006 (0.066, 0.089), **P < 0.001**	0.041 ± 0.006 (0.029, 0.053), **P < 0.001**
Gluteal	1.22 ± 0.10	1.24 ± 0.17	1.28 ± 0.14	0.022 ± 0.026 (−0.031, 0.074), *P* = 0.410	0.066 ± 0.021 (0.022, 0.109), **P = 0.004**	0.044 ± 0.028 (−0.013, 0.101), *P* = 0.123
Thigh	1.14 ± 0.19	1.12 ± 0.17	1.22 ± 0.19	0.031 ± 0.011 (0.011, 0.052), **P = 0.003**	0.080 ± 0.010 (0.060, 0.100), **P < 0.001**	0.049 ± 0.010 (0.029, 0.068), **P < 0.001**
Lower leg	1.33 ± 0.09	1.40 ± 0.09	1.42 ± 0.08	0.067 ± 0.012 (0.043, 0.092), **P < 0.001**	0.090 ± 0.024 (0.063, 0.117), **P < 0.001**	0.022 ± 0.011 (0.0, 0.045), **P = 0.046**
Foot	1.15 ± 0.13	1.14 ± 0.21	1.14 ± 0.26	−0.003 ± 0.052 (−0.113, 0.108), *P* = 0.957	−0.002 ± 0.078 (−0.017, 0.016), *P* = 0.977	0.0 ± 0.051 (−0.011, 0.011), *P* = 0.992
f ($*10^{-1}$)						
All muscles	1.57 ± 0.64	1.69 ± 0.51	1.76 ± 0.49	1.15 ± 0.26 (0.65, 1.66), **P < 0.001**	1.82 ± 0.30 (1.22, 2.41), **P < 0.001**	0.67 ± 0.21 (0.26, 1.07), **P = 0.001**
Gluteal	1.82 ± 0.53	1.75 ± 0.43	1.79 ± 0.45	−0.68 ± 1.12 (−2.98, 1.61), P = 0.551	−0.26 ± 0.85 (−1.98. 1.47)., *P* = 0.765	0.42 ± 3.94 (−1.00, 1.84), *P* = 0.551
Thigh	1.94 ± 0.58	1.98 ± 0.50	1.88 ± 0.54	0.41 ± 0.47 (−0.51, 1.33), *P* = 0.377	−0.59 ± 0.51 (−1.60, 0.42), *P* = 0.249	−1.00 ± 0.27 (−1.54, −0.46), **P < 0.001**
Lower leg	0.91 ± 0.31	1.20 ± 0.38	1.53 ± 0.46	2.93 ± 0.58 (1.77, 4.09), **P < 0.001**	6.23 ± 0.73 (4.77, 7.69), **P < 0.001**	3.30 ± 0.68 (1.94, 4.67), **P < 0.001**
Foot	1.25 ± 0.34	1.76 ± 0.47	2.18 ± 0.32	5.11 ± 1.26 (2.42, 7.80), **P = 0.001**	9.27 ± 1.07 (2.42, 7.80), **P < 0.001**	4.17 ± 1.40 (1.20, 7.15), **P = 0.009**
D* ($*10^{-2}$)						
All muscles	1.09 ± 0.48	1.22 ± 0.51	1.27 ± 0.50	0.13 ± 0.02 (0.09, 0.18), **P < 0.001**	0.18 ± 0.03 (0.13, 0.23), **P < 0.001**	0.05 ± 0.02 (0.00, 0.09), **P = 0.036**
Gluteal	1.16 ± 0.54	1.32 ± 0.55	1.22 ± 0.39	0.16 ± 0.06 (0.02, 0.29), **P = 0.022**	0.05 ± 0.07 (−0.09, 0.19), *P* = 0.466	−0.11 ± 0.08 (−0.26, 0.05), *P* = 0.171
Thigh	0.98 ± 0.32	1.03 ± 0.29	0.99 ± 0.29	0.05 ± 0.03 (−0.00, 0.11), *P* = 0.059	0.01 ± 0.03 (−0.04, 0.05), *P* = 0.778	−0.04 ± 0.03 (−0.09, 0.01), P = 0.079
Lower leg	1.19 ± 0.48	1.33 ± 0.50	1.59 ± 0.48	0.14 ± 0.07 (−0.00, 0.28), *P* = 0.052	0.40 ± 0.09 (0.22, 0.58), **P < 0.001**	0.26 ± 0.08 (0.09, 0.43), **P = 0.003**
Foot	0.79 ± 0.17	1.03 ± 0.31	1.29 ± 0.45	0.24 ± 0.07 (0.27 m 0.72), **P = 0.005**	0.49 ± 0.11 (0.27, 0.72), **P < 0.001**	0.26 ± 0.09 (0.06, 0.45), **P = 0.012**

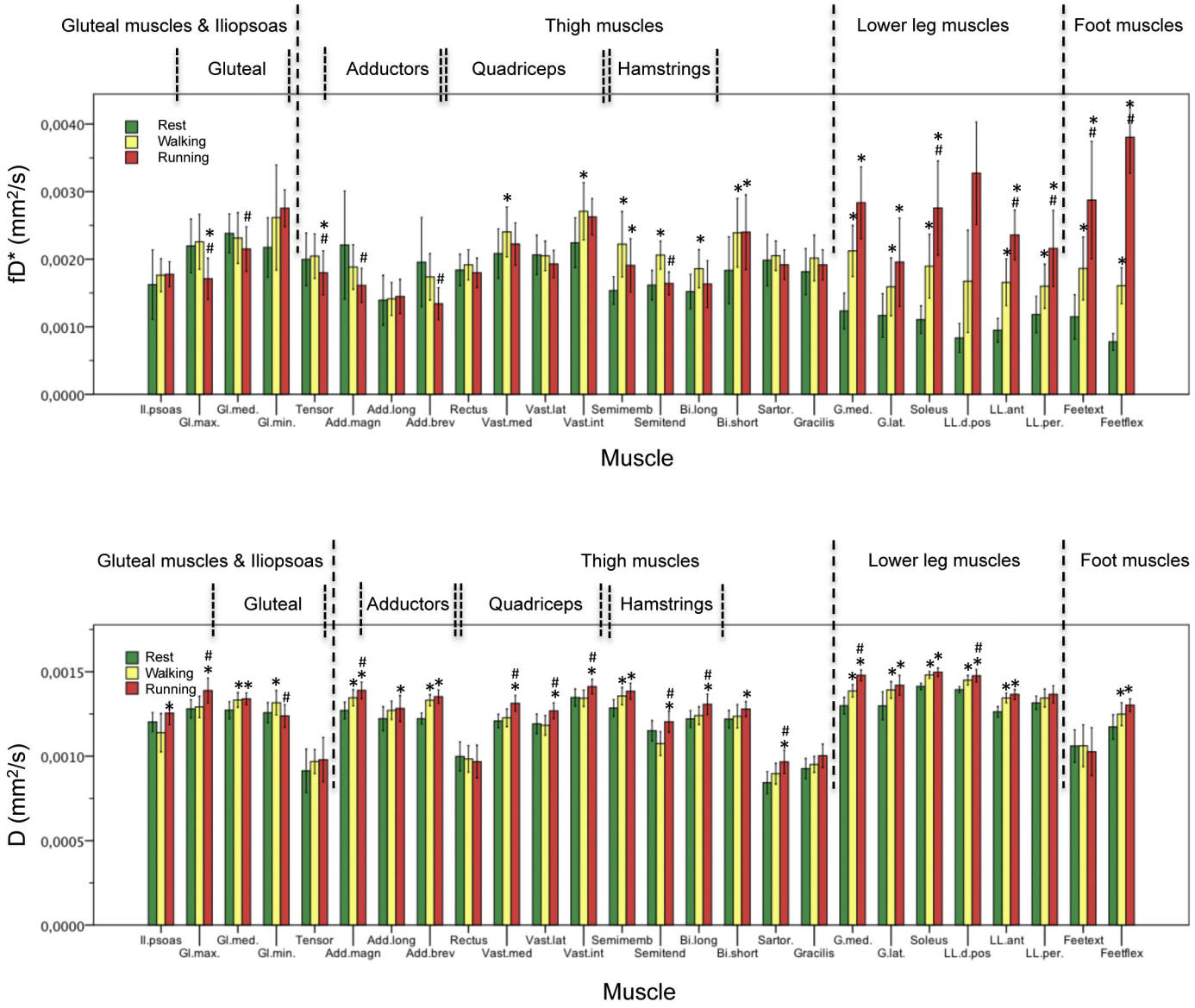

Fig. 2. Absolute fD* and D values of all muscles or muscle compartments. Il.psoas, Iliopsoas muscle; Gl.max., Gluteus maximus muscle; Gl.med, Gluteus medius muscle; Gl.min, Gluteus minimus muscle; Tensor, tensor fascia lata muscle; Add.magn, Adductor magnus muscle; Add.long, Adductor longus muscle; Add.brev, Adductor brevis muscle; Rectus, Rectus femoris muscle; Vast.med, Vastus medialis muscle; Vast.lat, Vastus lateralis muscle; Vast.int, Vastus intermedius muscle; Semimemb, Semimembranosus muscle; Semitend, Semitendinosus muscle; Bi.long, long head of biceps muscle; Bi.short, short head of biceps muscle; Sartor., Sartorius muscle; Gracilis, Gracilis muscle; G.med., Gastrocnemius medialis muscle; G.lat., Gastrocnemius lateralis muscle; Soleus, Soleus muscle; LL.d.pos, lower leg deep posterior compartment; LL.ant, lower leg anterior compartment; LL.per, lower leg peroneal compartment; Feetext, feet extensor muscles; Feetflex, feet flexor muscles.
* significantly different to “rest”
# significantly different to “walking”
Error bars: 95% confidence intervals.

parameters reverted to the resting values within 3 min during the recovery phase. This observation is in contrast to Filli et al. [19], who showed that the IVIM signal after muscle exercise remained significantly increased at least 20 min after exercise. In the present study, there was also no recovery of the calf during the scan time of 8 to 10 min, possibly due to the long activation time of the muscles prior to IVIM measurements.

No increase of fD* from walking to running was observed for the gluteal muscles, tensor fascia lata, quadriceps, hamstrings and adductor muscles. This observation is consistent with the well-known redistribution of blood flow during physical exercise in favor of the working muscles. For example, Bradley et al. [25] found in an asymmetric cycling exercise an increased blood flow to the cycling leg and a decrease in the contralateral non-cycling leg. Using IVIM, Nguyen et al. demonstrated an increase of the fD* parameter in the subscapularis muscle though activation via the lift-off test, while a decrease of the fD* in the non-active supraspinatus and infraspinatus muscle was observed [20]. In the present study, running initiated a redistribution of blood-flow towards the lower leg and foot.

On the other hand the iliopsoas, gluteal and thigh muscles (mainly the hamstrings) are more intensively activated only with higher speed in order to increase the stride frequency [26]; the running exercise performed in this experiment was only of moderate intensity. Although the tensor fascia lata is known as the “sprinter muscle”, it is not particularly active during running at a lower speed [27]. During running at a lower speed, the main forward movement is caused by the lower legs

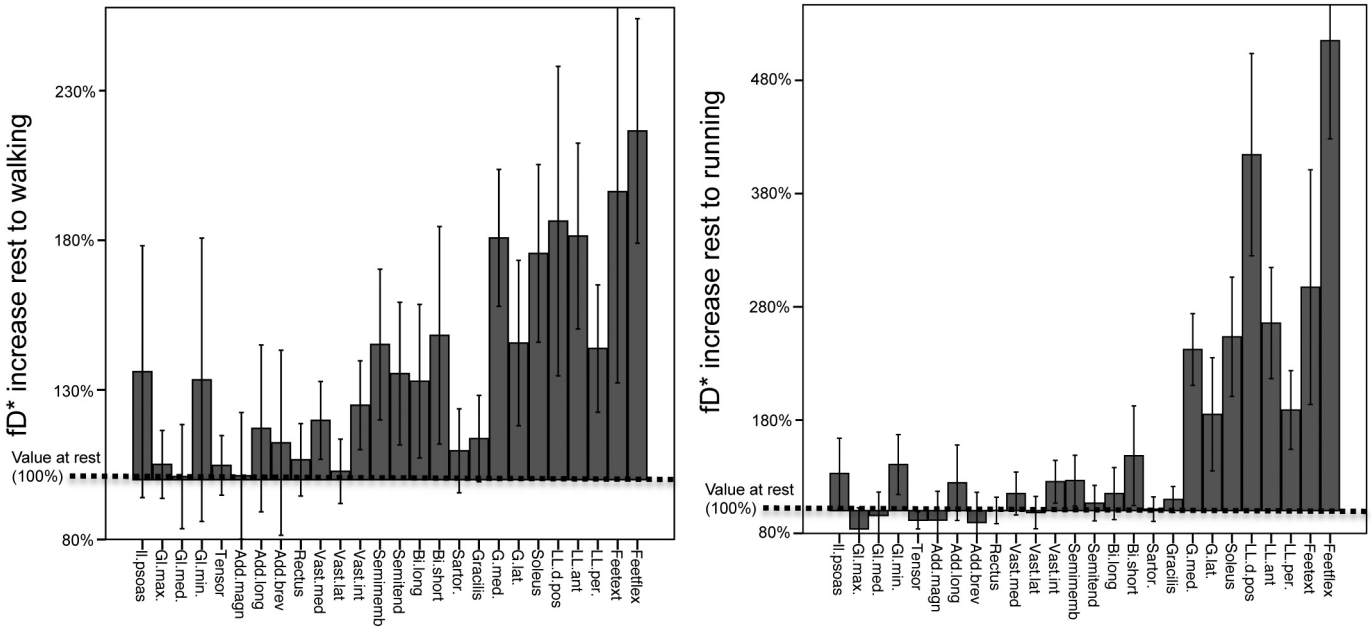

Fig. 3. Change of fD* through running as compared to rest. The relative value after running is presented as percentage of the value at rest (fD* value at rest equals 100%). Il.psoas, Iliopsoas muscle; Gl.max., Gluteus maximus muscle; Gl.med, Gluteus medius muscle; Gl.min, Gluteus minimus muscle; Tensor, tensor fascia lata muscle; Add.magn, Adductor magnus muscle; Add.long, Adductor longus muscle; Add.brev, Adductor brevis muscle; Rectus, Rectus femoris muscle; Vast.med, Vastus medialis muscle; Vast.lat, Vastus lateralis muscle; Vast.int, Vastus intermedius muscle; Semimemb, Semimembranosus muscle; Semitend, Semitendinosus muscle; Bi.long, long head of biceps muscle; Bi.short, short head of biceps muscle; Sartor., Sartorius muscle; Gracilis, Gracilis muscle; G.med., Gastrocnemius medialis muscle; G.lat., Gastrocnemius lateralis muscle; Soleus, Soleus muscle; LL.d.pos, lower leg deep posterior compartment; LL.ant, lower leg anterior compartment; LL.per, lower leg peroneal compartment; Feetext, feet extensor muscles; Feetflex, feet flexor muscles.
Error bars: 95% confidence intervals.

and feet; Up to a speed of ca. 25 km/h, the soleus and gastrocnemius contribute to vertical support in order to increase the stride length forces and hence increases the stride length [27]. Considering the smaller muscle size in the lower leg compared to the upper leg, the resulting force per unit muscle is extremely high.

The differences of the activation patterns between the thigh versus lower leg and foot muscles as well as between the different muscle groups may also be explained by the stance-phase and the swing-phase of the gait. The redistribution of blood towards the swing-phase muscles at the lower leg and food and the relatively low additional need of blood for the mostly stance-phase associated gluteal and thigh muscles may explain these findings. Awai et al. also found a proximal-distal imbalance in response to unloading [28]. Through the pre-swing phase, gastrocnemius and soleus undergo concentric activity and accelerate the trunk and leg forward while decelerating the downward motion of the trunk resulting in forward progression [29,30]. Around mid-stance the gastrocnemius and soleus net effect on the trunk and the leg is minor [30]. Neptune et al. described that the uniarticular knee (vastus) and hip extensor muscles (gluteus maximus) are critical to body support in the beginning of stance underlining their important stance-phase role, before the plantar flectors become active [30]. The hamstring muscles have a more complex role [30]. They decelerate the leg in late swing while accelerate the leg in the beginning of stance [30]. This is in line with findings of the present study, where the hamstrings had a higher activation during walking and running as had the quadriceps muscles.

Changes of the diffusion coefficient D in skeletal muscles after exercise has been observed in several other studies [19,21,31]. Besides

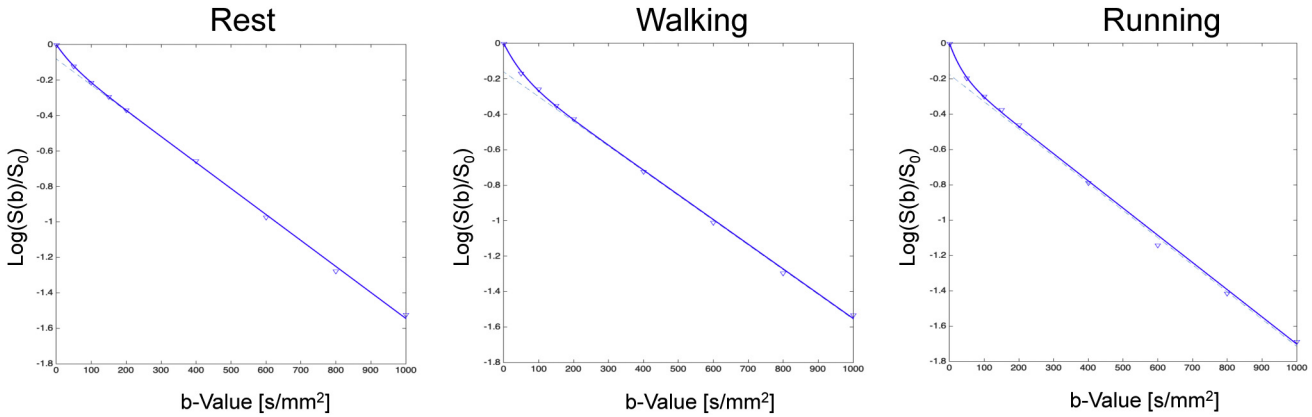

Fig. 4. Exemplary relative signal decay curve as a function of the b-value and the corresponding bi-exponential fit (blue line), measured in the soleus muscle of one volunteer. The dashed blue line corresponds to the mono-exponential fit for a b-value > 200 s/mm^2. The IVIM perfusion effect can be seen as deviation of the straight line from the blue line at low b-value. Note the gradual increase in steepness of the curve at low b values from rest to walking to running. (For interpretation of the references to colour in this figure legend, the reader is referred to the web version of this article.)

Table 2
Comparisons of different muscle subgroups regarding the change of IVIM measurements (in percent increase, %) from rest to walking, walking to running and rest to running. Mean difference ± SEM of the blood-flow values including 95% confidence intervals (CI; lower value, upper value) and P-values for the comparisons of the subgroups are provided for the perfusion parameter fD* and for the diffusion parameter D. *P*-values < 0.05 (in **bold**) are considered statistically significant.

	Change rest to walking (%)			Change walking to running (%)			Change rest to running (%)		
	Mean difference ± SEM (95% CI), P-value			Mean difference ± SEM (95% CI), P-value			Mean difference ± SEM (95% CI), P-value		
fD*									
Gluteal vs adductor muscles	2.9 ± 10.9	(−18.8, 24.6),	0.790	8.7 ± 6.9	(−5.0, 22.3),	0.211	4.8 ± 10.5	(−16.0, 25.7),	0.646
Quadriceps vs hamstring muscles	−21.9 ± 8.2	(−38.1, −5.7),	**0.009**	−0.7 ± 5.3	(−11.2, 9.8),	0.899	−19.9 ± 9.2	(−38.2, −1.7),	**0.033**
Vastus medialis vs lateralis	17.0 ± 7.9	(0.8, 32.1),	**0.040**	1.6 ± 10.0	(−1.9 22.1),	0.873	16.8 ± 11.1	(−5.9, 39.6),	0.142
Gastrocnemius medialis vs lateralis	35.1 ± 16.8	(0.7, 69.5),	**0.046**	4.0 ± 15.7	(−28.2, 36.1),	0.803	57.2 ± 27.8	(0.5, 113.9),	**0.048**
D									
Gluteal vs adductor muscles	−3.0 ± 1.4	(−5.8, −0.1),	**0.041**	−1.1 ± 1.4	(3.9, 1.7),	0.446	−4.2 ± 1.7	(−7.6, −8.1),	**0.016**
Quadriceps vs hamstring muscles	−2.3 ± 1.7	(−5.7, 1.1),	0.187	−1.0 ± 2.0	(−5.0, 3.0),	0.616	−3.3 ± 2.2	(−7.6, 1.0),	0.135
Vastus medialis vs lateralis	2.0 ± 2.5	(−3.1, 7.2),	0.424	−0.4 ± 1.8	(−4.1, 3.2),	0.813	1.7 ± 2.5	(−3.3, 6.7),	0.502
Gastrocnemius medialis vs lateralis	−1.3 3.7	(−8.8, 6.2),	0.724	4.2 ± 2.4	(−0.8, 9.1),	0.094	6.7 ± 4.0	(−1.6, 14.9),	0.108

being due to a slight increase in local temperature, the increase in the diffusion coefficient may be mainly due to an osmotically driven increase of interstitial water in contracting muscles [32]. This theory is in accordance with the significant changes observed in T2 weighted contrast in the muscle after exercise [33,34].

In the present study, we found an interesting negative correlation between changes in heart rate and changes in fD*, while no correlation of D with the heart rate was found. Those findings may relate to the previously reported dependence of fD* in the brain on the cardiac cycle. Similarly, no significant influence of the cardiac cycle on D was found for the brain [35]. Additionally, those heartrate dependent findings may reflect the training level of the individual volunteers: better trained individuals, with lower increases of the heart rate during the same activity also have a better “microvascular reserve of the muscles”, probably due to higher rates of microvessels, as shown in a histological study by Lee et al. [36]. Interestingly, this suggests that the IVIM method might be used to monitor the level of training of the microvascular reserve for example in athletes.

There are several limitations of this study. First, the number of volunteers was small ($n = 8$ volunteers, $n = 16$ legs). However, the retrospective power analysis revealed a minimum sample size of $n = 5$ for the main IVIM parameter fD*. Also the required sample sizes for the parameters f, D and D* were all < 12. Still, further investigations in larger cohort studies are needed to assess physiological and pathological muscle activation patterns. All volunteers were female. Moreover, although the volunteers walked or ran to the MR scanner and therefore finished the activity only just before the MR scan started, perfusion changes might have occurred during preparation and acquisition of the MR images. It is important to note that the region with the largest changes, the lower leg and foot, was scanned last. Finally, the IVIM MR method allows only for scanning post exercise, therefore no gait cycle dependent activation of the muscles could be determined.

5. Conclusions

In conclusion, the specific activation pattern of the muscles of lower limb during walking and running in human by using the non-invasive IVIM microvascular MR perfusion method was demonstrated.

Funding

CF was supported by the Swiss National Science Foundation.

Acknowledgements

The authors thank all technicians for their help regarding the acquisition of the MRI data.

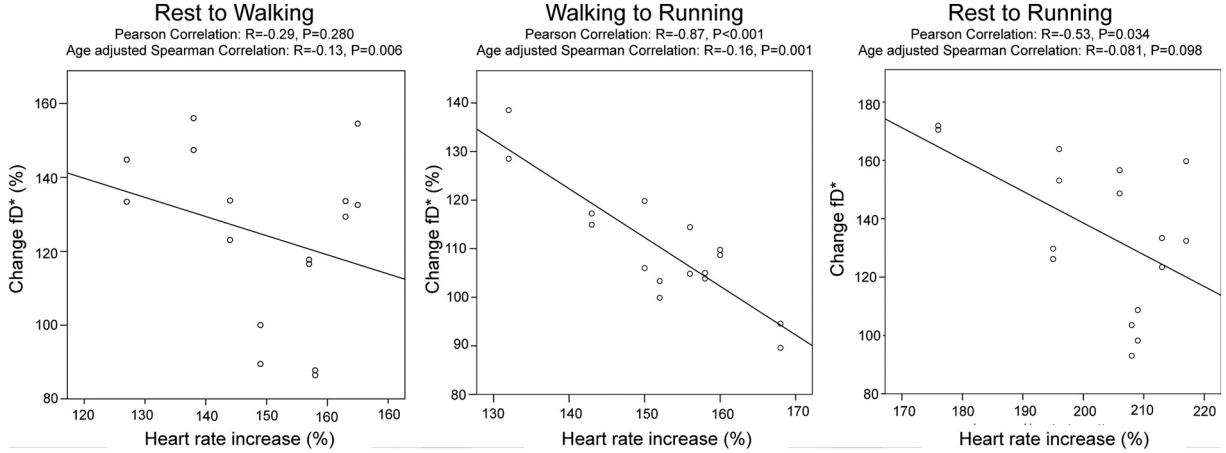

Fig. 5. Graphs demonstrating the inverse correlation of the increase of the heart rate (given as a relative value in percent) with the change of fD* (given as a relative value in percent) from rest to walking, walking to running, and rest to running, respectively.

Declaration of Competing Interest

No conflict of interest for any of the authors.

References

[1] Marsh RL, Ellerby DJ. Partitioning locomotor energy use among and within muscles. Muscle blood flow as a measure of muscle oxygen consumption. J Exp Biol 2006;209(Pt 13):2385–94.

[2] Marsh RL, Ellerby DJ, Carr JA, Henry HT, Buchanan CI. Partitioning the energetics of walking and running: swinging the limbs is expensive. Science 2004;303(5654):80–3.

[3] Sharafi A, Chang G, Regatte RR. Bi-component T1rho and T2 relaxation mapping of skeletal muscle in-vivo. Sci Rep 2017;7(1):14115.

[4] Bryant ND, Li K, Does MD, Barnes S, Gochberg DF, Yankeelov TE, et al. Multi-parametric MRI characterization of inflammation in murine skeletal muscle. NMR Biomed 2014;27(6):716–25.

[5] Maillard SM, Jones R, Owens C, Pilkington C, Woo P, Wedderburn LR, et al. Quantitative assessment of MRI T2 relaxation time of thigh muscles in juvenile dermatomyositis. Rheumatology (Oxford) 2004;43(5):603–8.

[6] Messer DJ, Bourne MN, Williams MD, Al Najjar A, Shield AJ. Hamstring muscle use in women during hip extension and the Nordic hamstring exercise: a functional magnetic resonance imaging study. J Orthop Sports Phys Ther 2018;48(8):607–12.

[7] Bourne M, Williams M, Pizzari T, Shield A. A functional MRI exploration of hamstring activation during the supine bridge exercise. Int J Sports Med 2018;39(2):104–9.

[8] Kinugasa R, Kawakami Y, Fukunaga T. Muscle activation and its distribution within human triceps surae muscles. J Appl Physiol (1985) 2005;99(3):1149–56.

[9] Jiji RS, Pollak AW, Epstein FH, Antkowiak PF, Meyer CH, Weltman AL, et al. Reproducibility of rest and exercise stress contrast-enhanced calf perfusion magnetic resonance imaging in peripheral arterial disease. J Cardiovasc Magn Reson 2013;15:14.

[10] Wu WC, Mohler 3rd E, Ratcliffe SJ, Wehrli FW, Detre JA, Floyd TF. Skeletal muscle microvascular flow in progressive peripheral artery disease: assessment with continuous arterial spin-labeling perfusion magnetic resonance imaging. J Am Coll Cardiol 2009;53(25):2372–7.

[11] Wong SM, Backes WH, Zhang CE, Staals J, van Oostenbrugge RJ, Jeukens C, et al. On the reproducibility of inversion recovery intravoxel incoherent motion imaging in cerebrovascular disease. AJNR Am J Neuroradiol 2018;39(2):226–31.

[12] Federau C. Intravoxel incoherent motion MRI as a means to measure in vivo perfusion: a review of the evidence. NMR Biomed 2017;30(11).

[13] Le Bihan D, Breton E, Lallemand D, Aubin ML, Vignaud J, Laval-Jeantet M. Separation of diffusion and perfusion in intravoxel incoherent motion MR imaging. Radiology 1988;168(2):497–505.

[14] Federau C, O'Brien K, Meuli R, Hagmann P, Maeder P. Measuring brain perfusion with intravoxel incoherent motion (IVIM): initial clinical experience. J Magn Reson Imaging 2014;39(3):624–32.

[15] Le Bihan D, Breton E, Lallemand D, Grenier P, Cabanis E, Laval-Jeantet M. MR imaging of intravoxel incoherent motions: application to diffusion and perfusion in neurologic disorders. Radiology 1986;161(2):401–7.

[16] Morvan D. In vivo measurement of diffusion and pseudo-diffusion in skeletal muscle at rest and after exercise. Magn Reson Imaging 1995;13(2):193–9.

[17] Qi J, Olsen NJ, Price RR, Winston JA, Park JH. Diffusion-weighted imaging of inflammatory myopathies: polymyositis and dermatomyositis. J Magn Reson Imaging 2008;27(1):212–7.

[18] Karampinos DC, King KF, Sutton BP, Georgiadis JG. Intravoxel partially coherent motion technique: characterization of the anisotropy of skeletal muscle microvasculature. J Magn Reson Imaging 2010;31(4):942–53.

[19] Filli L, Boss A, Wurnig MC, Kenkel D, Andreisek G, Guggenberger R. Dynamic intravoxel incoherent motion imaging of skeletal muscle at rest and after exercise. NMR Biomed 2015;28(2):240–6.

[20] Nguyen A, Ledoux JB, Omoumi P, Becce F, Forget J, Federau C. Selective microvascular muscle perfusion imaging in the shoulder with intravoxel incoherent motion (IVIM). Magn Reson Imaging 2017;35:91–7.

[21] Nguyen A, Ledoux JB, Omoumi P, Becce F, Forget J, Federau C. Application of intravoxel incoherent motion perfusion imaging to shoulder muscles after a lift-off test of varying duration. NMR Biomed 2016;29(1):66–73.

[22] Mastropietro A, Porcelli S, Cadioli M, Rasica L, Scalco E, Gerevini S, et al. Triggered intravoxel incoherent motion MRI for the assessment of calf muscle perfusion during isometric intermittent exercise. NMR Biomed 2018;31(6):e3922.

[23] Federau C, Maeder P, O'Brien K, Browaeys P, Meuli R, Hagmann P. Quantitative measurement of brain perfusion with intravoxel incoherent motion MR imaging. Radiology 2012;265(3):874–81.

[24] Anderson FC, Pandy MG. Individual muscle contributions to support in normal walking. Gait Posture 2003;17(2):159–69.

[25] Bradley SE, Childs AW, Combes B, Cournand A, Wade OL, Wheeler HO. The effect of exercise on the splanchnic blood flow and splanchnic blood volume in normal man. Clin Sci 1956;15(3):457–63.

[26] Duteil S, Bourrilhon C, Raynaud JS, Wary C, Richardson RS, Leroy-Willig A, et al. Metabolic and vascular support for the role of myoglobin in humans: a multi-parametric NMR study. Am J Physiol Regul Integr Comp Physiol 2004;287(6):R1441–9.

[27] Dorn TW, Schache AG, Pandy MG. Muscular strategy shift in human running: dependence of running speed on hip and ankle muscle performance. J Exp Biol 2012;215(Pt 11):1944–56.

[28] Awai L, Franz M, Easthope CS, Vallery H, Curt A, Bolliger M. Preserved gait kinematics during controlled body unloading. J Neuroeng Rehabil 2017;14(1):25.

[29] Neptune RR, Kautz SA, Zajac FE. Contributions of the individual ankle plantar flexors to support, forward progression and swing initiation during walking. J Biomech 2001;34(11):1387–98.

[30] Neptune RR, Zajac FE, Kautz SA. Muscle force redistributes segmental power for body progression during walking. Gait Posture 2004;19(2):194–205.

[31] Sasaki M, Sumi M, Van Cauteren M, Obara M, Nakamura T. Intravoxel incoherent motion imaging of masticatory muscles: pilot study for the assessment of perfusion and diffusion during clenching. AJR Am J Roentgenol 2013;201(5):1101–7.

[32] Sjogaard G, Adams RP, Saltin B. Water and ion shifts in skeletal muscle of humans with intense dynamic knee extension. Am J Physiol 1985;248(2 Pt 2):R190–6.

[33] Fisher MJ, Meyer RA, Adams GR, Foley JM, Potchen EJ. Direct relationship between proton T2 and exercise intensity in skeletal muscle MR images. Invest Radiol 1990;25(5):480–5.

[34] Fleckenstein JL, Canby RC, Parkey RW, Peshock RM. Acute effects of exercise on MR imaging of skeletal muscle in normal volunteers. AJR Am J Roentgenol 1988;151(2):231–7.

[35] Federau C, Hagmann P, Maeder P, Muller M, Meuli R, Stuber M, et al. Dependence of brain intravoxel incoherent motion perfusion parameters on the cardiac cycle. PLoS One 2013;8(8):e72856.

[36] Lee HJ, Rha SY, Chung YE, Shim HS, Kim YJ, Hur J, et al. Tumor perfusion-related parameter of diffusion-weighted magnetic resonance imaging: correlation with histological microvessel density. Magn Reson Med 2014;71(4):1554–8.